Obstructive sleep apnea–hypopnea results in significant variations in cerebral hemodynamics detected by diffuse optical spectroscopies

Obstructive sleep apnea–hypopnea results in significant variations in cerebral hemodynamics detected by diffuse optical spectroscopies

Yajun Hou[1,2,7]**, Yu Shang**[1,7]**, Ran Cheng**[1]**, Youquan Zhao**[1,3]**,
Yanli Qin**[1,2]**, Richard Kryscio**[4]**, Abner Rayapati**[5]**,
Don Hayes Jr**[6] **and Guoqiang Yu**[1,8]

[1] Department of Biomedical Engineering, University of Kentucky, Lexington, KY 40506, USA
[2] College of Science, Shenyang Ligong University, Shenyang, Liaoning 110159, People's Republic of China
[3] Department of Biomedical Engineering, Tianjin University, Tianjin 300072, People's Republic of China
[4] Department of Statistics, University of Kentucky, Lexington, KY 40536, USA
[5] Department of Psychiatry, University of Kentucky, Lexington, KY 40509, USA
[6] College of Medicine, The Ohio State University, Columbus, OH 43210, USA

E-mail: guoqiang.yu@uky.edu

Abstract

The objective of this study was to adapt a novel near-infrared diffuse correlation spectroscopy (DCS) flow-oximeter for simultaneous and continuous monitoring of relative changes in cerebral blood flow (rCBF) and cerebral oxygenation (i.e. oxygenated/deoxygenated/total hemoglobin concentration: $\Delta[HbO_2]/\Delta[Hb]/\Delta THC$) during overnight nocturnal polysomnography (NPSG) diagnostic test for obstructive sleep apnea–hypopnea (OSAH). A fiber-optic probe was fixed on subject's frontal head and connected to the DCS flow-oximeter through a custom-designed fiber-optic connector, which allowed us to easily connect/detach the optical probe from the device when the subject went to bathroom. To minimize the disturbance to the subject, the DCS flow-oximeter was remotely operated by a desktop located in the control room. The results showed that apneic events caused significant variations in rCBF and ΔTHC. Moreover, the degrees of variations in all measured cerebral variables were significantly correlated with the severity of

[7] These authors contributed equally to this work
[8] Author to whom all correspondence should be addressed.

OSAH as determined by the apnea–hypopnea index (AHI), demonstrating the OSAH influence on both CBF and cerebral oxygenation. Large variations in arterial blood oxygen saturation (SaO_2) were also found during OSAH. Since frequent variations/disturbances in cerebral hemodynamics may adversely impact brain function, future study will investigate the correlations between these cerebral variations and functional impairments for better understanding of OSAH pathophysiology.

Keywords: near-infrared diffuse correlation spectroscopy (DCS) flow-oximeter, cerebral blood flow (CBF), cerebral blood oxygenation, obstructive sleep apnea–hypopnea (OSAH), apnea–hypopnea index (AHI), nocturnal polysomnography (NPSG)

(Some figures may appear in colour only in the online journal)

1. Introduction

Obstructive sleep apnea–hypopnea (OSAH) affects an estimated 15 million adult Americans (Khayat *et al* 2008, Somers *et al* 2008). OSAH is characterized by repetitive episodes of upper airway obstruction during sleep that disturb sleep architecture and induce intermittent hypoxia (Khayat *et al* 2008, McGinley *et al* 2008, Schwartz *et al* 2008, Somers *et al* 2008, Reichmuth *et al* 2009). OSAH causes daytime hypersomnia and drowsiness, memory loss, and neuro-cognitive impairment and has been associated with hypertension, cardiovascular diseases, stroke, and diabetes (Guilleminault *et al* 1983, Partinen and Guilleminault 1990, Palomaki 1991, Guilleminault and Suzuki 1992, Reichmuth *et al* 2005). The standard diagnostic test for OSAH is nocturnal polysomnography (NPSG) in a sleep laboratory (Rosen *et al* 2012). Diagnosis is determined by the apnea–hypopnea index (AHI) (Rosen *et al* 2012), which is the total number of apneas and hypopne as observed per hour of sleep.

Apneic events during OSAH are associated with surges in blood pressure, arterial blood oxygen saturation (SaO_2), and cerebral blood hemodynamics (Safonova *et al* 2003, Olopade *et al* 2007, Urbano *et al* 2008). Decreases in cerebral oxygenation during OSAH, for example, have been observed using near-infrared spectroscopy (NIRS) (Safonova *et al* 2003, Olopade *et al* 2007, Pizza *et al* 2010). Impairment in cerebral metabolism has also been found using magnetic resonance spectroscopy (MRS) in patients with OSAH (Kamba *et al* 2001, O'Donoghue *et al* 2005). Recurrent perturbations by OSAH may adversely affect cerebral autoregulation (Urbano *et al* 2008), a tightly controlled mechanism to maintain cerebral blood flow (CBF) during blood pressure fluctuations. Cerebral autoregulation impairment increases the risk of cerebral ischemia/hypoxia (Foster *et al* 2007), which may induce neuropsychological deficits (e.g. excessive daytime sleepiness, cognitive impairment, behavioral problems) (Kim *et al* 1997). Taken together, recurrent OSAH during sleep may result in impairments in CBF autoregulation, cerebral oxygenation, and oxygen metabolism, leading to neuropsychological deficits and cerebral dysfunction.

The study of hemodynamic variations/disturbances during OSAH as well as the complex interactions among different hemodynamic parameters may reveal new insights about their impacts on brain since cerebral hemodynamic/metabolic parameters are usually coupled and interactive (Ances *et al* 2008, Shin *et al* 2008). However, most of the current researches have been limited to evaluating cerebral hemodynamic/metabolic impairment in a *single* parameter (i.e. blood flow, blood oxygenation or oxygen metabolic rate) (Hayakawa *et al* 1996, Hausser-Hauw *et al* 2000, Kamba *et al* 2001, Safonova *et al* 2003, Olopade *et al* 2007). Therefore,

there is a critical need for a high-throughput, portable and easy-to-use device to continuously track the perturbations/variations in multiple cerebral hemodynamic parameters during OSAH at the bedside of sleep room.

Unfortunately, noninvasive techniques for making continuous measurements of multiple cerebral hemodynamic parameters at the bedside during sleep are rare. transcranial Doppler (TCD) ultrasound can measure cerebral blood flow velocity (CBFV) in the major arteries supplying the brain. However, only the proximal portions of the intracranial arteries can be insonated by TCD and there is an inconsistent relationship between proximal arterial flow velocity and CBF (Edlow *et al* 2010). The only available noninvasive method for tracking cerebral blood oxygenation at the bedside is NIRS.

Our laboratory has been working on the development of various NIRS-based techniques for tissue hemodynamic measurements. Particularly, we have constructed and validated a portable dual-wavelength diffuse correlation spectroscopy (DCS) flow-oximeter, which has the capability to measure both blood flow and oxygenation of tissue noninvasively (Shang *et al* 2009, Shang *et al* 2011a, 2011b, Yu *et al* 2011, Dong *et al* 2012b, He *et al* 2013, Li *et al* 2013). The objective of this study was to adapt this new technology for simultaneous and continuous monitoring of multiple cerebral hemodynamic parameters during overnight sleep in subjects with OSAH. These measured parameters included relative changes in CBF (rCBF), oxy-hemoglobin concentration ($\Delta[HbO_2]$), deoxy-hemoglobin concentration ($\Delta[Hb]$) and derived total hemoglobin concentration ($\Delta THC = \Delta[HbO_2] + \Delta[Hb]$). We then quantified the perturbations/variations in these hemodynamic parameters during OSA compared to the NPSG testing results.

2. Methods and materials

2.1. Participants

Sixteen (16) adults participated in this study with signed consent forms approved by the University of Kentucky (UK) Institutional Review Board. The study was conducted in the UK Good Samaritan Hospital Sleep Disorders Center. Subjects underwent continuously overnight NPSG testing in conjunction with cerebral hemodynamic monitoring by our novel DCS flow-oximeter (see section 2.2), while they were sleeping for their diagnostic NPSG testing.

Three out of the 16 subjects were excluded from our data analysis since the optical probe fell off from the heads of two subjects and NPSG system did not work properly in testing one subject. Table 1 reports the characteristics of the remaining 13 subjects with valid data. The sequence of the subjects in this table was based on the value of AHI in the order from lowest to highest.

2.2. Near-infrared (NIR) DCS flow-oximeter

We used a custom-designed dual-wavelength DCS flow-oximeter (see figure 1(*b*)) to continuously monitor rCBF, $\Delta[HbO_2]$, $\Delta[Hb]$, and ΔTHC during overnight sleep. Details about the DCS flow-oximeter can be found elsewhere (Shang *et al* 2009). Briefly, long-coherence (>5 m) NIR lights emitted from two laser diodes (785 and 854 nm, ~100 mw, Crystalaser Inc., NV, USA) are delivered alternately to tissues via two multimode source fibers (diameter of each fiber=200 μm). The scattered light through the tissue is collected by a single-mode detector fiber (diameter=5.6 μm) connected to an avalanche photodiode (APD, PerkinElmer Inc., Canada). The source and detector fibers are placed on the tissue surface at a distance ranging from millimeters to centimeters depending on the penetration depth required (Chance *et al*

Table 1. Subject characteristics.

Subject	Sex	Age (years)	AHI[a]	BMI[b] ($kg\,m^{-2}$)	MLS[c] (%)	TST[d] (min)	SEI[e]
S1	F	72	1.4	52	91	343.5	71.7
S2	M	58	3.0	24	95	258.0	75.9
S3	M	61	3.4	32	84	356.0	76.1
S4	F	57	4.1	48	85	351.5	74.8
S5	M	30	12.0	29	88	481.5	90.0
S6	F	43	14.3	25	93	222.5	86.7
S7	F	64	14.7	27	86	417.0	84.9
S8	F	61	15.8	47	71	243.5	46.9
S9	M	56	23.5	34	97	286.0	58.0
S10	M	54	33.7	38	83	397.0	77.5
S11	M	42	58.9	56	87	360.5	74.0
S12	M	54	68.0	34	81	262.0	53.4
S13	F	42	74.3	63	80	460.0	90.9
Average		53.4 ± 11.3	25.2 ± 25.7	39.2 ± 12.7	86.2 ± 7.0	341.5 ± 83.3	73.9 ± 13.7

[a] Apnea hypopnea index.
[b] Body mass index.
[c] Mean lowest SaO_2.
[d] Total sleep time.
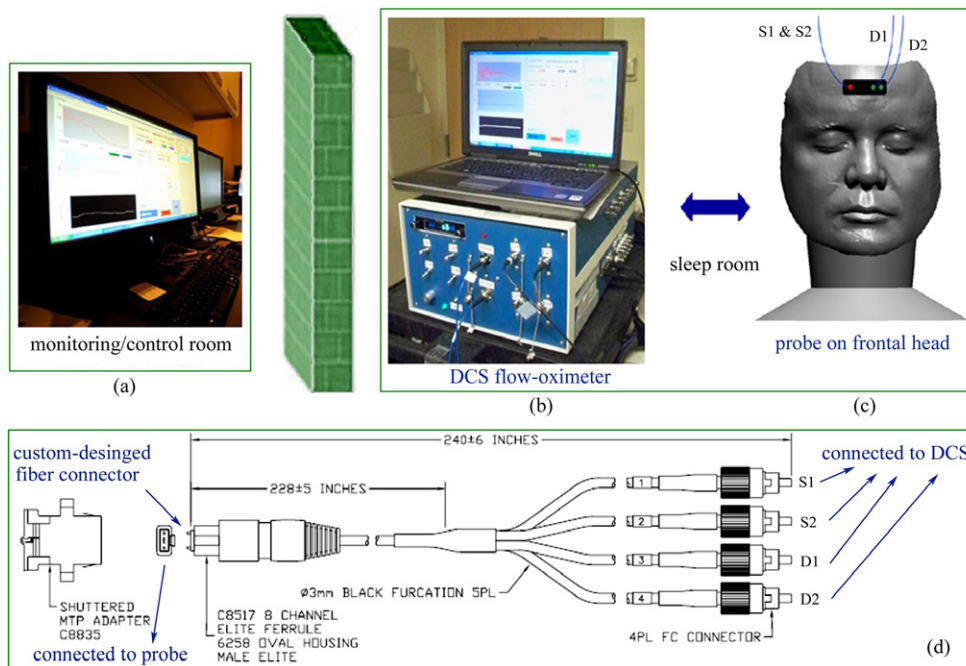[e] Sleep efficiency index.

Figure 1. Experimental setup: remotely controlled desktop in the control room (*a*). DCS flow-oximeter and control panel (laptop) in the sleep room (*b*). Fiber-optic probe installed on subject's frontal head. Two source fibers (S1 and S2) were bundled and placed in the same location and two detector fibers (D1 and D2) were placed at 2.5 and 3.0 cm respectively away from the source fibers (*c*). Source and detector fibers connected to the custom-designed fiber-optic connector (*d*).

1992, van Beekvelt *et al* 2001). The light intensity fluctuation within a single speckle area of tissue (~25 μm^2), collected by the single-mode fiber and detected by the APD, is sensitive to the motion of moving scatterers in tissue (primarily red blood cells). An autocorrelator board (correlator.com, NJ, USA) takes the output of APD and computes the light intensity temporal autocorrelation function. The electric field temporal autocorrelation function $G_1(\tau)$ derived from the measured normalized light intensity autocorrelation function satisfies the correlation diffusion equation in highly scattering media (Boas *et al* 1995, Boas and Yodh 1997, Dong *et al* 2012a). For the case of diffusive motion of moving scatterers, the normalized electric field temporal autocorrelation function $g_1(\tau)$ decays at an early time approximately exponentially in τ (delay time). A blood flow index (BFI) is thus extracted by fitting the $g_1(\tau)$ curve whose decay rate depends on a parameter α (which is proportional to the tissue blood volume fraction) and the motion of red blood cells (Boas *et al* 1995, Cheung *et al* 2001, Yu *et al* 2005a, 2005b). rCBF is defined as the percentage change of BFI relative to its baseline value (assigned to be '1'). Two flow curves are generated by the two wavelength measurements (785 and 854 nm). Previous studies have shown that DCS flow measurements are not sensitive to wavelength (Shang *et al* 2009, Shang *et al* 2013). Therefore, rCBF derived from one wavelength (785 nm) is used in this study for data analysis.

The oxygenation information is extracted from data obtained by recording the average light intensities at two wavelengths (785 and 854 nm) detected by the APD. Using the known extinction coefficients of major chromophores (i.e. HbO$_2$ and Hb) and differential pathlength factors (DPFs) at corresponding wavelengths (Duncan *et al* 1995, Kim *et al* 2005), the modified Beer–Lambert law is applied to determine Δ[HbO$_2$] and Δ[Hb] relative to their baseline values (assigned to be '0' μM).

2.3. Experimental protocols and data collection

The subject was asked to lie supine on the sleep bed and a video camera was used to remotely monitor the patient activities in the sleep room. Standard PSG sensors were installed on the body for simultaneous monitoring of multiple physiological parameters including nasal airflow and SaO$_2$. For the optical measurements of cerebral hemodynamic parameters, a fiberoptic probe (figure 1(*c*)) was taped on the middle of subject's frontal head. A self-adhesive elastic band was then employed around the forehead to secure the probe and minimize the influence of room light on optical measurements. Inside the probe, two source fibers were bundled together for delivering the lights at two wavelengths alternatively and two detector fibers were arranged at 2.5 and 3.0 cm from the source fibers. The probe was connected to a 4-channel DCS flow-oximeter for the measurements of rCBF and cerebral oxygenation changes during sleep. To reduce the influence of cerebral hemodynamic heterogeneity, it is crucial to keep the probe on the same region of subject's head for continuous monitoring of overnight changes in cerebral hemodynamics. For this purpose, a special fiber-optic connector was designed (Fiberoptic Systems Inc., CA, USA, see figure 1(*d*)) to detach the probe fibers from our DCS device when the subject went to bathroom. To minimize the disturbance to the subject, we remotely operated the optical instrument and marked all events (e.g. motion artifacts) from a control room. DCS flow-oximeter and its control panel (laptop, figure 1(*b*)) were kept inside the sleep room and remotely operated by a desktop located in the control room (figure 1(*a*)). The two computers (i.e. the laptop and desktop) worked under the 'remote desktop connect' mode in the Microsoft Windows Operating System (Dong *et al* 2012b) and communicated through the internal network in the Sleep Disorder Center. Optical data were continuously recorded during overnight sleep at a sampling rate of 0.5 Hz.
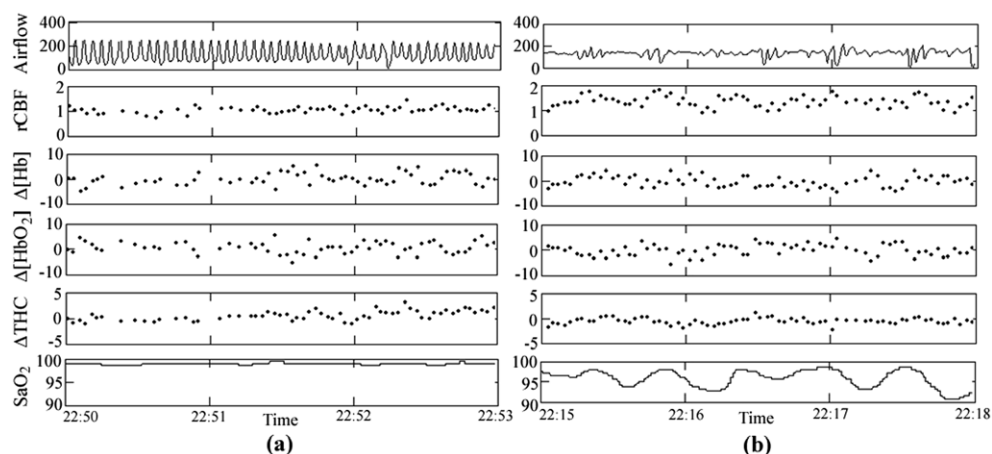
Figure 2. Time course data of nasal airflow (μv mm^{-1}), rCBF, Δ[HbO$_2$] (μM), Δ[Hb] (μM), ΔTHC (μM), and SaO$_2$ (%) in an illustrative subject (S10) during OSAH-off (*a*) and during OSAH-on (*b*). The airflow data demonstrated a normal breathing pattern when there was no OSAH (*a*). By contrast, OSAH resulted in repetitive episodes of airway obstruction (*b*). Among all measured hemodynamic variables, rCBF and SaO$_2$ showed larger variations during OSAH-on (*b*) compared to those during OSAH-off (*a*).

2.4. Data analysis

The penetration depth of NIR light depends on the tissue optical properties and source–detector (S–D) separation, and is roughly half of the S–D separation (van Beekvelt *et al* 2001). Although larger S–D separation (e.g. 3.0 cm) results in deeper penetration depth, DCS data collected from 2.5 cm S–D separation were found in this study to have sufficient signal-to-noise ratio (SNR) for data analysis. The S–D separation of 2.5 cm for the detection of CBF and cerebral oxygenation was previously validated and has been broadly used in various human brain studies (Durduran *et al* 2004, Li *et al* 2005, Durduran *et al* 2009, Edlow *et al* 2010, Kim *et al* 2010, Shang *et al* 2011b, Cheng *et al* 2012).

From the overnight optical measurements, we observed large baseline shifts in the measured variables over the long recording periods (several hours). This is not unusual as many factors could result in the baseline shift such as changes in body temperature, body posture, and sleeping stage. However, the baseline shift makes it difficult to quantitatively determine hemodynamic differences during the time segments with or without OSAH. As such, we used the 'detrend' function in MATLAB (Mathworks Inc., MA, USA) to remove the baseline shifts and then compared the differences in hemodynamic variations (standard deviations) between the apneic events and normal respirations. For the comparison, we need to identify and separate the time segments with or without OSAH. OSAH is characterized by repetitive episodes of airflow reduction (hypopnea) or cessation (apnea) due to upper airway collapse during sleep. The time segments were thus characterized according to the feature of nasal airflow measured by NPSG. Figure 2 shows different patterns during normal breath (*a*) and apnea/hypopnea (*b*). Based on the criteria reported in literature (Millman *et al* 1995), apnea was defined as a cessation of airflow lasting more than 10 s, while hypopnea was defined as a decrease in airflow for more than 10 s resulting in a >4% fall in SaO$_2$. Both hypopnea and apnea periods were identified as OSAH-on compared to normal respirations as OSAH-off. Notably, based on the NPSG testing results (body motion) and

our observations (video monitoring) in the control room, data with motion artifacts during OSAH were excluded from our analysis as they may result in the overestimation of tissue blood flow (Shang *et al* 2010, Gurley *et al* 2012).

It was found that the spans of these time segments varied substantially ranging from minutes to hours, and hemodynamic variations (standard deviations) were associated with the time spans. To standardize, we divided the segment longer than 2 min (with or without OSAH) into multiple sub-segments with a constant time interval of 2 min. We then calculated the standard deviation (SD) in each sub-segment (2 min) for each subject. The mean ± standard deviation of the SDs over all sub-segments was used to characterize the hemodynamic perturbation/variation for each subject.

The mean values of the two serials of datasets (i.e. OSAH-on and OSAH-off) over all subjects were calculated, resulting in 13 paired mean values of SDs. Paired t-test was then applied to examine the difference between the paired mean values. A paired t-test based on 13 subjects has 80% power to detect an effect size of 0.85 or larger. Stepwise linear regression analysis was used to investigate the correlations between hemodynamic variations and NPSG variables including Age, AHI, body mass index (BMI), mean lowest SaO_2 (MLS), total sleep time (TST), and sleep efficiency index (SEI). Here, SEI is defined as the ratio of TST to the time in bed. A multiple regression model based on 13 subjects and two predictor variables has 80% power to show significance provided these predictors explain at least 50% of the total variability in the dependent variable.

We also grouped the subjects based on the AHI values (Bixler *et al* 1998, Shamsuzzaman *et al* 2002); Group 1 included S1 to S4 with AHI < 5 (healthy controls) and Group 2 included S5 to S13 with AHI ≥ 5 (patients with OSAH). Two sample t-tests were used to examine the group differences in hemodynamic variations and NPSG variables. Statistical significance was defined at the 0.05 level throughout.

3. Results

3.1. Individual time course data

Figure 2 shows illustrative data of nasal airflow, rCBF, Δ[HbO$_2$], Δ[Hb], ΔTHC, and SaO_2 in two segments (OSAH-off (*a*) and OSAH-on (*b*)) measured from a representative subject (S10). The airflow data demonstrated a normal breathing pattern when there was no OSAH (Figure 2(*a*)). By contrast, OSAH resulted in repetitive episodes of airway obstruction (Figure 2(*b*)). Among all measured hemodynamic variables, rCBF and SaO_2 showed larger variations during OSAH-on compared to those during OSAH-off.

3.2. Comparison of hemodynamic variations between OSAH-on and OSAH-off

Figure 3 shows the comparison results of each individual for hemodynamic variations (SDs) between the segments during OSAH-on and during OSAH-off. The majority of subjects (*n* ≥8) had larger mean variations (SDs) in rCBF (figure 3(*a*)), ΔTHC (figure 3(*d*)), and SaO_2 (figure 3(*e*)) during OSAH-on compared to those during OSAH-off. By contrast, there were no consistent trends/patterns in the mean SDs of Δ[HbO$_2$] (figure 3(*b*)) and Δ[Hb] (figure 3(*c*)) between the two serials of datasets (i.e. OSAH-on and OSAH-off).

The averaged results over all subjects (figure 4) also demonstrated the same patterns as described above, that is, the SDs of rCBF, ΔTHC and SaO_2 during OSAH-on were significantly ($p < 0.01$, paired *t*-test) larger than those during OSAH-off.
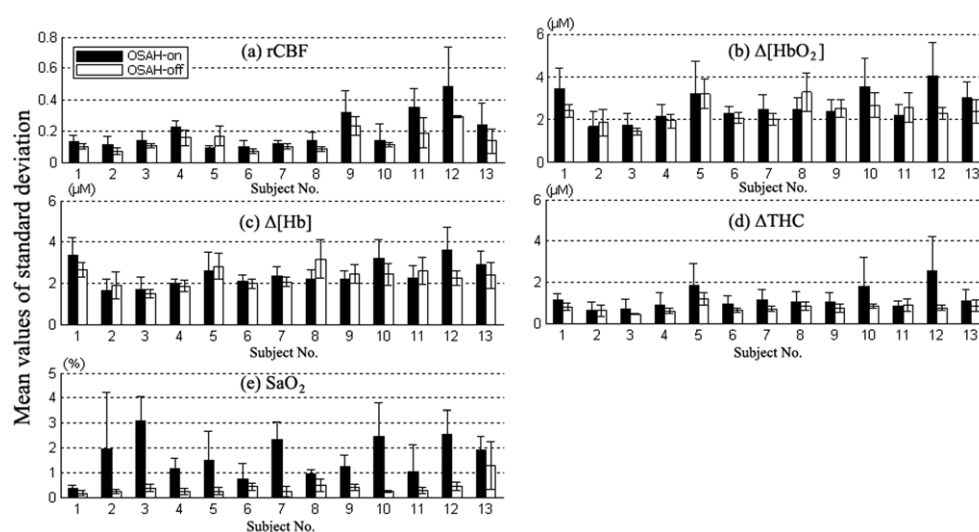
Figure 3. Comparison of hemodynamic variations (standard deviations) between OSAH-on and OSAH-off in each individual: rCBF (*a*), Δ[HbO$_2$] (*b*), Δ[Hb] (*c*), ΔTHC (*d*), and SaO$_2$ (*e*). The solid and empty bars represent mean values of standard deviations in the segments with OSAH-on and OSAH-off, respectively. Note that the mean SDs of rCBF (*a*), ΔTHC (*d*), and SaO$_2$ (*e*) during OSAH-on were larger than those during OSAH-off in the majority of subjects ($n \geqq 8$).
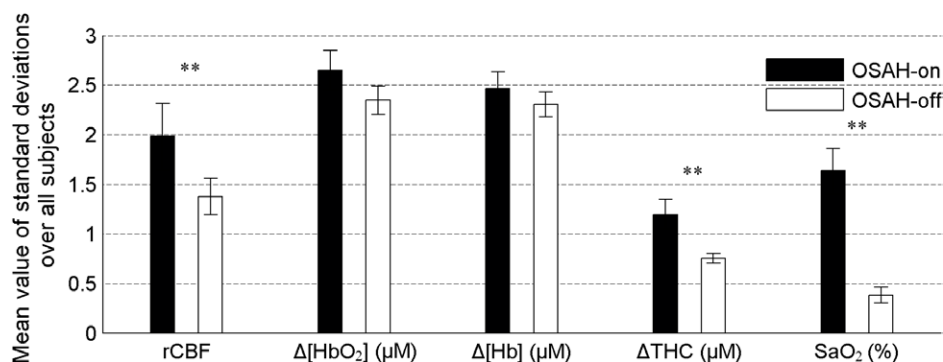

Figure 4. Comparison of the mean values over all subjects (*n*=13) in hemodynamic variations (standard variations) between the two serials of datasets (OSAH-on versus OSAH-off). The solid and empty bars represent the datasets with and without OSAH, respectively. The asteroids represent that hemodynamic variations during OSAH-on are significantly larger than those during OSAH-off. Note that the scales in *y*-axis for different hemodynamic variables are not same due to different units, thus the variation amplitudes may not be visually comparable. For better visualization, rCBF values were magnified by 10 times. On average over subjects (*n*=13), the SDs of rCBF, ΔTHC and SaO$_2$ during OSAH-on were found to be significantly larger than those during OSAH-off.

3.3. Correlations between hemodynamic variations and NPSG testing variables

Table 2 lists the correlation results by stepwise regression analysis. Here, the positive or negative coefficients with $p < 0.05$ indicate significant positive or negative correlations, respectively. rCBF variations were significantly correlated with AHI (coefficient = 0.0033)

Table 2. Stepwise linear regression analysis.

Hemodynamic variations	Coefficients	*T* statistics	*P* values
rCBF variations			
AHI	0.0033	4.2388	0.0017
AGE (years)			
BMI ($kg\,m^{-2}$)			
MLS (%)			
TST (min)			
SEI	−0.0038	−2.6251	0.0254
R^2	0.72		
p value	0.0016		
$\Delta[HbO_2]$ variations (μM)			
AHI	0.0216	3.0828	0.0116
AGE (years)			
BMI (kg/m^2)	−0.0352	−2.4834	0.0324
MLS (%)			
TST (min)			
SEI			
R^2	0.52		
p value	0.0253		
$\Delta[Hb]$ variations (μM)			
AHI	0.0191	3.2416	0.0018
AGE (years)			
BMI ($kg\,m^{-2}$)	−0.0275	−2.3080	0.0437
MLS (%)			
TST (min)			
SEI			
R^2	0.53		
p value	0.0229		
ΔTHC variations (μM)			
AHI	0.0156	2.8330	0.0178
AGE (years)			
BMI ($kg\,m^{-2}$)	−0.0268	−2.4071	0.0369
MLS (%)			
TST (min)			
SEI			
R^2	0.49		
p value	0.0355		

and negatively correlated with SEI (coefficient = −0.0038). The variations of $\Delta[HbO_2]$, $\Delta[Hb]$, and ΔTHC were significantly correlated with AHI (coefficient = 0.0216, 0.0191, 0.0156) and negatively correlated with BMI (coefficient = −0.0352, −0.0275, −0.0268).

3.4. Differences in hemodynamic variations and NPSG testing variables between the two groups with different AHIs

No significant differences were found for all hemodynamic variations and NPSG testing variables between the patient group (AHI ≥ 5, *n*=9) and healthy group (AHI < 5, *n*=4). This is likely due to the small group sizes (power ranged from 5–16%).

4. Discussion and conclusions

Previous studies have shown that the recurrence of OSAH during sleep induces surges in blood pressure, SaO_2, and cerebral hemodynamics/metabolism that may lead to neuropsychological deficits and cerebral dysfunction (Kamba *et al* 2001, Safonova *et al* 2003, Olopade *et al* 2007, Urbano *et al* 2008). Continuous and simultaneous monitoring of brain physiology

during sleep would provide important insights for better understanding of the OSAH impact on brain. To date, only a few studies have used NIRS to continuously monitor cerebral blood oxygenation during overnight NPSG testing (Hayakawa *et al* 1996, Hausser-Hauw *et al* 2000, Olopade *et al* 2007). In those studies, lower levels of cerebral oxygenation and SaO_2 were observed in patients with OSAH. In the present study we demonstrated *for the first time* the feasibility of adapting the novel dual-wavelength DCS flow-oximeter (see figure 1(*b*)) to continuously monitor both CBF and cerebral oxygenation variations during overnight NPSG tests in patients with OSAH. To ensure cerebral measurements in the same region of brain, a special fiber-optic connector (see figures 1(*c*) and (*d*)) was designed to connect or disconnect the optical probe (fixed on subject's head) from the optical device when the subject went to bathroom. To minimize the disturbance to the subject in the sleep room, the optical instrument was remotely operated by a desktop located in the control room (see figure 1(*a*)). The longitudinal and continuous monitoring of multiple physiological parameters in brain during overnight sleep allowed us to investigate the impacts of OSAH on cerebral hemodynamics and the interactions among these measured parameters.

Among the measured multiple cerebral hemodynamic variables (see figure 2), we observed lager variations in rCBF and ΔTHC during periods of apnea (OSAH-on) compared to periods of normal respirations (OSAH-off) in the majority of subjects (see figure 3). Consequentially, average variations for all subjects were significantly larger during OSAH-on (see figure 4). The large variations in rCBF and ΔTHC (proportional to blood volume change) were likely due to the OSAH-induced hypercapnic/hypocapnic effect (i.e. CO_2 increase/decrease), which is known to result in cerebrovascular dilation/constriction (Poulin *et al* 1996, Severinghaus and Lassen 1967). The average variations in cerebral oxygenation (i.e. $\Delta[HbO_2]$ and $\Delta[Hb]$) during OSAH-on were also larger than those during OSAH-off, although the differences did not reach statistical significance (see figure 4). Stepwise regression analysis (see table 2) demonstrated that the degrees of variations in all cerebral variables (i.e. rCBF, $\Delta[HbO_2]$, $\Delta[Hb]$, and ΔTHC) were significantly correlated with the severity of OSAH (i.e. AHI), indicating OSAH is influencing both CBF and cerebral oxygenation. In addition, OSAH also resulted in significantly larger variations in SaO_2 during OSAH (see figures 3 and 4), which is consistent with previous findings (Safonova *et al* 2003).

No significant differences in cerebral hemodynamic variations were observed between the healthy controls (*n*=4) and the patients with OSAH (*n*=9), which is likely due to the small numbers of subjects in both groups. However, that fact that degrees of variations in all cerebral variables were significantly correlated with the severity of OSAH (see table 2) demonstrates the sensitivity of our optical measurements in evaluation of OSAH impacts on cerebral hemodynamics.

Some other factors were also found to be associated with cerebral hemodynamic variations during OSAH, including SEI and BMI. For example, the degree of rCBF variations was negatively correlated with SEI, indicating that a stable rCBF benefited from efficient sleep. We speculate that the 'partial value effect' may be the reason why BMI negatively affected the degrees of variations in $\Delta[HbO_2]$, $\Delta[Hb]$ and ΔTHC. The brain signals detected by NIRS/DCS are generally influenced by the overlying tissue (i.e. skin, fat, skull), i.e. 'partial volume effect' (Durduran *et al* 2004). The degree of partial volume effect depends on the thickness of overlying tissues which may differ among subjects with different values of BMI. Subjects with higher BMI usually have increased thicknesses of overlying tissue, leading to larger partial volume effects on the detected cerebral signals. This may explain why the subjects with larger values of BMI tended to have smaller variations in cerebral oxygenation. To verify this hypothesis, future study will measure the thickness of overlying tissue in subjects using other imaging modalities (e.g. MRI) and investigate the relationship between the thickness and BMI. To minimize the partial volume effect, multiple S–D separations (ranging from small

to large, e.g. 0.5–3 cm) could be used to detect and separate cerebral signals from overlying tissues (Yu *et al* 2005a, Durduran and Yodh 2013).

One limitation of this study is the penetration depth of NIRS/DCS measurements. Although the separation of 2.5 cm has been broadly used in NIRS/DCS measurements to detect cerebral hemodynamics in brain cortex (Durduran *et al* 2004, Li *et al* 2005, Durduran *et al* 2009, Edlow *et al* 2010, Kim *et al* 2010, Shang *et al* 2011b, Cheng *et al* 2012), larger separations are desirable in order to study deeper brain tissue noninvasively. In order to obtain sufficient signals at large S–D separations, future study may combine multiple detector fibers in one location and average these signals to improve the SNR (Cheng *et al* 2012, Gurley *et al* 2012).

Another constraint of this study is the baseline shifts observed in the measured cerebral variables during overnight measurements (several hours), which makes it difficult to quantitatively determine cerebral hemodynamic changes induced by OSAH. Instead, we removed the baseline shifts and compared the differences in cerebral hemodynamic variations (standard deviations) between the apneic events and normal respirations. Nevertheless, quantification of cerebral hemodynamic disturbances induced by OSAH is of importance for understanding of OSAH impacts on brain function.

In conclusion, we have successfully adapted a novel dual-wavelength DCS flow-oximeter for continuous and longitudinal monitoring of CBF and cerebral oxygenation during OSAH to investigate the OSAH impacts on the brain. DCS flow-oximeter demonstrated sensitivity to track dynamic variations in both CBF and cerebral oxygenation during OSAH. We found that apneic events induced large variations in cerebral hemodynamics and the degrees of these variations were correlated with the severity of OSAH. Since large and frequent variations/disturbances in cerebral hemodynamics during OSAH may adversely impact brain function, future study will quantify cerebral function (e.g. memory loss, neurocognitive impairment) in patients with OSAH and investigate the correlations between cerebral hemodynamic variations during OSAH and functional impairments for better understanding of OSAH pathophysiology.

Acknowledgments

References

Ances B M, Leontiev O, Perthen J E, Liang C, Lansing A E and Buxton R B 2008 Regional differences in the coupling of cerebral blood flow and oxygen metabolism changes in response to activation: Implications for BOLD-fMRI *Neuroimage* **39** 1510–21

Bixler E O, Vgontzas A N, Ten Have T, Tyson K and Kales A 1998 Effects of age on sleep apnea in men: I. Prevalence and severity *Am. J. Respir. Crit. Care Med.* **157** 144–8

Boas D A, Campbell L E and Yodh A G 1995 Scattering and imaging with diffusing temporal field correlations *Phys. Rev. Lett.* **75** 1855–8

Boas D A and Yodh A G 1997 Spatially varying dynamical properties of turbid media probed with diffusing temporal light correlation *J. Opt. Soc. Am. A* **14** 192–215

Chance B, Dait M T, Zhang C, Hamaoka T and Hagerman F 1992 Recovery from exercise-induced desaturation in the quadriceps muscles of elite competitive rowers *Am. J. Physiol.* **262** C766–75

Cheng R, Shang Y, Hayes D, Saha S P and Yu G 2012 Noninvasive optical evaluation of spontaneous low frequency oscillations in cerebral hemodynamics *Neuroimage* **62** 1445–54

Cheung C, Culver J P, Takahashi K, Greenberg J H and Yodh A G 2001 *In vivo* cerebrovascular measurement combining diffuse near-infrared absorption and correlation spectroscopies *Phys. Med. Biol.* **46** 2053–65

Dong J, Bi R Z, Ho J H, Thong P S P, Soo K C and Lee K 2012a Diffuse correlation spectroscopy with a fast Fourier transform-based software autocorrelator *J. Biomed. Opt.* **17** 097004

Dong L, Kudrimoti M, Cheng R, Shang Y, Johnson E L, Stevens S D, Shelton B J and Yu G 2012b Noninvasive diffuse optical monitoring of head and neck tumor blood flow and oxygenation during radiation delivery *Biomed. Opt. Express* **3** 259–72

Duncan A, Meek J H, Clemence M, Elwell C E, Tyszczuk L, Cope M and Delpy D T 1995 Optical pathlength measurements on adult head, calf and forearm and the head of the newborn infant using phase resolved optical spectroscopy *Phys. Med. Biol.* **40** 295–304

Durduran T and Yodh A G 2013 Diffuse correlation spectroscopy for non-invasive, micro-vascular cerebral blood flow measurement *Neuroimage* **85** 51–63

Durduran T, Yu G, Burnett M G, Detre J A, Greenberg J H, Wang J J, Zhou C and Yodh A G 2004 Diffuse optical measurement of blood flow, blood oxygenation, and metabolism in a human brain during sensorimotor cortex activation *Opt. Lett.* **29** 1766–8

Durduran T *et al* 2009 Transcranial optical monitoring of cerebrovascular hemodynamics in acute stroke patients *Opt. Express* **17** 3884–902

Edlow B L, Kim M N, Durduran T, Zhou C, Putt M E, Yodh A G, Greenberg J H and Detre J A 2010 The effects of healthy aging on cerebral hemodynamic responses to posture change *Physiol. Meas.* **31** 477–95

Foster G E, Hanly P J, Ostrowski M and Poulin M J 2007 Effects of continuous positive airway pressure on cerebral vascular response to hypoxia in patients with obstructive sleep apnea *Am. J. Respir. Crit. Care Med.* **175** 720–5

Guilleminault C, Connolly S J and Winkle R A 1983 Cardiac arrhythmia and conduction disturbances during sleep in 400 patients with sleep apnea syndrome *Am. J. Cardiol.* **52** 490–4

Guilleminault C and Suzuki M 1992 Sleep-related hemodynamics and hypertension with partial or complete upper airway obstruction during sleep *Sleep* **15** S20–4

Gurley K, Shang Y and Yu G 2012 Noninvasive optical quantification of absolute blood flow, blood oxygenation, and oxygen consumption rate in exercising skeletal muscle *J. Biomed. Opt.* **17** 075010

Hausser-Hauw C, Rakotonanahary D and Fleury B 2000 Obstructive-sleep apnea syndrome: brain oxygenation measured with near-infrared spectroscopy. Preliminary results *Neurophysiol. Clin.* **30** 113–8

Hayakawa T, Terashima M, Kayukawa Y, Ohta T and Okada T 1996 Changes in cerebral oxygenation and hemodynamics during obstructive sleep apneas *Chest* **109** 916–21

He L, Lin Y, Shang Y, Shelton B J and Yu G 2013 Using optical fibers with different modes to improve the signal-to-noise ratio of diffuse correlation spectroscopy flow-oximeter measurements *J. Biomed. Opt.* **18** 037001

Kamba M, Inoue Y, Higami S, Suto Y, Ogawa T and Chen W 2001 Cerebral metabolic impairment in patients with obstructive sleep apnoea: an independent association of obstructive sleep apnoea with white matter change *J. Neurol. Neurosurg. Psychiatry* **71** 334–9

Khayat R, Patt B and Hayes D Jr 2009 Obstructive sleep apnea: the new cardiovascular disease. Part I: obstructive sleep apnea and the pathogenesis of vascular disease *Heart Fail. Rev.* **14** 143–53

Kim H C, Young T, Matthews C G, Weber S M, Woodward A R and Palta M 1997 Sleep-disordered breathing and neuropsychological deficits. A population-based study *Am. J. Respir. Crit. Care Med.* **156** 1813–9

Kim J G, Xia M N and Liu H L 2005 Extinction coefficients of hemoglobin for near-infrared spectroscopy of tissue *IEEE Eng. Med. Biol. Mag.* **24** 118–21

Kim M N *et al* 2010 Noninvasive measurement of cerebral blood flow and blood oxygenation using near-infrared and diffuse correlation spectroscopies in critically brain-Injured adults *Neurocrit. Care* **12** 173–80

Li J, Dietsche G, Iftime D, Skipetrov S E, Maret G, Elbert T, Rockstroh B and Gisler T 2005 Noninvasive detection of functional brain activity with near-infrared diffusing-wave spectroscopy *J. Biomed. Opt.* **10** 44002

Li T, Lin Y, Shang Y, He L, Huang C, Szabunio M and Yu G 2013 Simultaneous measurement of deep tissue blood flow and oxygenation using noncontact diffuse correlation spectroscopy flow-oximeter *Sci. Rep.* **3** 1358

McGinley B M, Schwartz A R, Schneider H, Kirkness J P, Smith P L and Patil S P 2008 Upper airway neuromuscular compensation during sleep is defective in obstructive sleep apnea *J. Appl. Physiol.* **105** 197–205

Millman R P, Carlisle C C, McGarvey S T, Eveloff S E and Levinson P D 1995 Body fat distribution and sleep apnea severity in women *Chest* **107** 362–6

O'Donoghue F J, Briellmann R S, Rochford P D, Abbott D F, Pell G S, Chan C H, Tarquinio N, Jackson G D and Pierce R J 2005 Cerebral structural changes in severe obstructive sleep apnea *Am. J. Respir. Crit. Care Med.* **171** 1185–90

Olopade C O, Mensah E, Gupta R, Huo D Z, Picchietti D L, Gratton E and Michalos A 2007 Noninvasive determination of brain tissue oxygenation during sleep in obstructive sleep apnea: a near-infrared spectroscopic approach *Sleep* **30** 1747–55

Palomaki H 1991 Snoring and the risk of ischemic brain infarction *Stroke* **22** 1021–5

Partinen M and Guilleminault C 1990 Daytime sleepiness and vascular morbidity at 7 year follow-up in obstructive sleep apnea patients *Chest* **97** 27–32

Pizza F, Biallas M, Wolf M, Werth E and Bassetti C L 2010 Nocturnal cerebral hemodynamics in snorers and in patients with obstructive sleep apnea: a near-infrared spectroscopy study *Sleep* **33** 205–10

Poulin M J, Liang P J and Robbins P A 1996 Dynamics of the cerebral blood flow response to step changes in end-tidal PCO2 and PO2 in humans *J. Appl. Physiol.* **81** 1084–95

Reichmuth K J, Austin D, Skatrud J B and Young T 2005 Association of sleep apnea and type II diabetes: a population-based study *Am. J. Respir. Crit. Care Med.* **172** 1590–5

Reichmuth K J, Dopp J M, Barczi S R, Skatrud J B, Wojdyla P, Hayes D and Morgan B J 2009 Impaired vascular regulation in patients with obstructive sleep apnea *Am. J. Respir. Crit. Care Med.* **180** 1143–50

Rosen C L, Auckley D, Benca R, Foldvary-Schaefer N, Iber C, Kapur V, Rueschman M, Zee P and Redline S 2012 A multisite randomized trial of portable sleep studies and positive airway pressure autotitration versus laboratory-based polysomnography for the diagnosis and treatment of obstructive sleep apnea: the home pap study *Sleep* **35** 757–67

Safonova L P, Michalos A, Wolf U, Choi J H, Wolf M, Mantulin W W, Hueber D M and Gratton E 2003 Diminished cerebral circulatory autoregulation in obstructive sleep apnea investigated by near-infrared spectroscopy *Sleep Res. Online* **5** 123–32

Schwartz A R, Patil S P, Laffan A M, Polotsky V, Schneider H and Smith P L 2008 Obesity and obstructive sleep apnea: pathogenic mechanisms and therapeutic approaches *Proc. Am. Thorac. Soc.* **5** 185–92

Severinghaus J W and Lassen N 1967 Step hypocapnia to separate arterial from tissue PCO2 in the regulation of cerebral blood flow *Circ. Res.* **20** 272–8

Shamsuzzaman A S, Winnicki M, Lanfranchi P, Wolk R, Kara T, Accurso V and Somers V K 2002 Elevated C-reactive protein in patients with obstructive sleep apnea *Circulation* **105** 2462–4

Shang Y, Chen L, Toborek M and Yu G 2011a Diffuse optical monitoring of repeated cerebral ischemia in mice *Opt. Express* **19** 20301–15

Shang Y, Cheng R, Dong L, Ryan S J, Saha S P and Yu G 2011b Cerebral monitoring during carotid endarterectomy using near-infrared diffuse optical spectroscopies and electroencephalogram *Phys. Med. Biol.* **56** 3015–32

Shang Y, Lin Y, Henry B A, Cheng R, Huang C, Chen L, Shelton B J, Swartz K R, Salles S S and Yu G 2013 Noninvasive evaluation of electrical stimulation impacts on muscle hemodynamics via integrating diffuse optical spectroscopies with muscle stimulator *J. Biomed. Opt.* **18** 105002

Shang Y, Symons T B, Durduran T, Yodh A G and Yu G 2010 Effects of muscle fiber motion on diffuse correlation spectroscopy blood flow measurements during exercise *Biomed. Opt. Express* **1** 500–11

Shang Y, Zhao Y, Cheng R, Dong L, Irwin D and Yu G 2009 Portable optical tissue flow oximeter based on diffuse correlation spectroscopy *Opt. Lett.* **34** 3556–8

Shin H K, Nishimura M, Jones P B, Ay H, Boas D A, Moskowitz M A and Ayata C 2008 Mild induced hypertension improves blood flow and oxygen metabolism in transient focal cerebral ischemia *Stroke* **39** 1548–55

Somers V K *et al* 2008 Sleep apnea and cardiovascular disease—An American Heart Association/American College of Cardiology Foundation Scientific Statement from the American Heart Association Council for High Blood Pressure Research Professional Education Committee, Council on Clinical Cardiology, Stroke Council, and Council on Cardiovascular Nursing *J. Am. Coll. Cardiol.* **52** 686–717

Urbano F, Roux F, Schindler J and Mohsenin V 2008 Impaired cerebral autoregulation in obstructive sleep apnea *J. Appl. Physiol.* **105** 1852–7

van Beekvelt M C P, Colier W N J M, Wevers R A and van Engelen B G M 2001 Performance of near-infrared spectroscopy in measuring local O-2 consumption and blood flow in skeletal muscle *J. Appl. Physiol.* **90** 511–9

Yu G, Durduran T, Lech G, Zhou C, Chance B, Mohler E R and Yodh A G 2005a Time-dependent blood flow and oxygenation in human skeletal muscles measured with noninvasive near-infrared diffuse optical spectroscopies *J. Biomed. Opt.* **10** 024027

Yu G, Durduran T, Zhou C, Wang H W, Putt M E, Saunders H M, Sehgal C M, Glatstein E, Yodh A G and Busch T M 2005b Noninvasive monitoring of murine tumor blood flow during and after photodynamic therapy provides early assessment of therapeutic efficacy *Clin. Cancer. Res.* **11** 3543–52

Yu G, Shang Y, Zhao Y, Cheng R, Dong L and Saha S P 2011 Intraoperative evaluation of revascularization effect on ischemic muscle hemodynamics using near-infrared diffuse optical spectroscopies *J. Biomed. Opt.* **16** 027004